J Mater Sci (2011) 46:1253–1258
DOI 10.1007/s10853-010-4905-6

Influence of fabrication method on the structure and thermal expansion property of $ZrWMoO_8$ and its composites

Qin-Qin Liu · Xiao-Nong Cheng · Juan Yang ·
Xiu-Juan Sun

Received: 25 May 2010 / Accepted: 6 September 2010 / Published online: 21 September 2010

Abstract We report the preparation of $ZrWMoO_8$ and its composites with near zero thermal expansion property using in situ solid state reaction or co-precipitation route. The aim of this study is to compare the influence of the fabrication method on the structure and thermal expansion of the products. The composition of the obtained powders was characterized by X-ray diffraction (XRD) and thermal expansion property was investigated by Thermomechanical Analysis (TMA), respectively. The results indicate that the room temperature structure of $ZrWMoO_8$ depends on the preparation method, and the structure can be indexed either as α-ZrW_2O_8 structure for in situ solid state reaction or as β-ZrW_2O_8 structure for co-precipitation route. The participation of the water in the reaction process was speculated to be the reason for the difference structure. However, no matter which structure $ZrWMoO_8$ adopted, it exhibits excellent negative thermal expansion property and can be utilized to decrease the thermal expansion of ZrO_2. The only difference is that the CTE curves of ZrO_2 composites with $ZrWMoO_8$ adopting α-ZrW_2O_8 structure have a discontinuity at about 150 °C due to the α–β phase transition while the other curves are linear.

Introduction

Negative thermal expansion (NTE) compounds are useful for producing composites that have no or very low thermal expansion. Some silicates such as eucriptite and spodumen [1, 2] and some titanates [3] are found to show NTE property. However, NTE in these materials is generally restricted to very narrow temperatures and is anisotropic. In 1996, cubic ZrW_2O_8 was found to show isotropic NTE from 0.3 to 1050 K [4], this material has the potential to make composites with no expansion and is expected to be used widely in the electronic and ceramic industries.

However, there are some drawbacks to this material. One is the order–disorder (α to β) phase transition around 433 K, which changes the linear coefficient of thermal expansion (CTE) from -8.8 to $-4.7 \times 10^{-6}\ K^{-1}$ [5, 6]. This discontinuity does exist in the thermal expansion curve of ZrO_2/ZrW_2O_8 composite [7, 8], which might cause thermal stress and makes ZrW_2O_8 difficult to be commercially used. Another is a phase transition to an orthorhombic structure (γ-ZrW_2O_8) at 0.21 GPa [9] that leads to invalidation during the processing of the Cu/ZrW_2O_8 composites [10]. Furthermore, finite element analysis finds that ZrW_2O_8-containing composites can have stresses in excess of the material strength [11]. These defects might be improved by substituting Mo for W in ZrW_2O_8, which could reduce the order–disorder phase transition temperature under room temperature (200 K for $ZrWMoO_8$) and increase the compression resistance [12–14].

Although $ZrWMoO_8$ with linear CTE above room temperature is more suitable for practical application, there is not any report on utilizing it to fabricate composites with near zero CTE until now. The dehydration precursor method [15] is the most utilized synthesis method, but

---

Electronic supplementary material The online version of this article (doi:10.1007/s10853-010-4905-6) contains supplementary material, which is available to authorized users.

Q.-Q. Liu (✉) · X.-N. Cheng · J. Yang · X.-J. Sun
School of Materials Science and Engineering, Jiangsu University, Zhenjiang, Jiangsu, People's Republic of China
e-mail: liu_qin_qin@126.com

resulted $ZrWMoO_8$ can not be utilized as an additive to decrease thermal expansion as it shows abnormal positive thermal expansion property (PTE) at room temperature [16]. It is found that the existence of the water is the reason for the abnormal PTE, in this study, $ZrWMoO_8$ and its composites with ZrO_2 were first synthesized by in situ solid state method to refrain from drawing into the water. For comparison, co-precipitation route was also utilized to fabricate $ZrWMoO_8$ and its composites, the influence of the preparation method on the structure and thermal expansion properties of the $ZrWMoO_8$ and its composites were studied.

Experimental

Preparation of $ZrWMoO_8$ and it composites by in situ solid state method

Analytical reagent chemical agents (ZrO_2, WO_3, and Mo O_3, including ammonium tungstate ($N_5H_{37}W_6O_{24}\cdot H_2O$), ammonium molybdate ($N_5H_{37}Mo_6O_{24}\cdot H_2O$) used in co-precipitation method) purchased from raw Sinopharm Chemical Reagent Co., Ltd were used as raw materials. ZrO_2, WO_3, and MoO_3 were weighted at different weight ratios listed in the Table 1, and mixed with a little ethanol. Then, the mixture was milled in an agate ball mill for 24 h to reduce the mean size, followed by calcination at 600 °C for 4 h, at 800 °C for 8 h, then at 900 °C for 12 h with intermittent ground for 40 min. After that, the obtained powders were cold pressed into a cylinder at 20 Mpa with the size of $\Phi 5 \times 30$ mm and sintered at 1020 °C for 1.5 h in air in a hermetical Pt crucible with a cover, then quenched in cold water.

Preparation of $ZrWMoO_8$ and it composites by co-precipitation route

Zirconium oxynitrate [$ZrO(NO_3)_2\cdot 5H_2O$, 99%, Zibo Rongruida Micro Materials Plant, China], $N_5H_{37}W_6O_{24}\cdot H_2O$, and $N_5H_{37}Mo_6O_{24}\cdot H_2O$ were weighted according to ratio listed in the Table 2. Zr, W, and Mo solution were prepared by dissolving the above raw materials in distilled water separately, the W solution and Mo solution were mixed, and then the mixture solution and Zr solution were added at the same time to the 25-mL distilled water under vigorous stirring, a white precipitate was produced. Stirring the above mixture for another 2 h, aging for 12 h, and drying at 80 °C, the white precursor was obtained. Then, these precursor powders were calcined at 600 °C for 4 h, cooled in air, ground, pressed, and sintered in the same way as above method.

Table 1 The mass of raw materials applied in in situ solid state reaction method

Sample	Composition	ZrO_2 (g)	WO_3 (g)	MoO_3 (g)
G1	α-$ZrWMoO_8$	12.322	23.184	14.395
G2	α-$ZrWMoO_8$/60 wt% ZrO_2	18.713	8.694	5.398
G3	α-$ZrWMoO_8$/33 wt% ZrO_2	14.990	9.272	5.758
G4	α-$ZrWMoO_8$/25 wt% ZrO_2	12.913	9.272	5.758

Experimental techniques

The specimens were characterized by X-ray Powder diffraction (XRD) using Rigaku D/max2500 (Cu$K\alpha_1$ 1.54059 Å, 40 kV, 200 mA, 10–50°, 5°/min). The thermal expansion coefficients were measured by thermomechanical analysis (TMA) using NETZSCH DIL 402EP. The microstructure was observed by scanning electron microscope (SEM) using JSM-7001F JEOL. The composition was analyzed by energy dispersive spectrometer (EDS) using OXFORD INCA.

Results and discussion

Sample G1 as prepared by in situ solid state method is calcined at different temperatures to determine a proper sintering temperature, the XRD patterns of the resulted products are shown in Fig. 1. As we can see, the product obtained after calcination at 600 °C is the mixture of ZrO_2, WO_3, and MoO_3 (Fig. 1a), indicating no chemical reaction happened. Further heating at 800 °C yields trigonal $ZrWMoO_8$ (Fig. 1b) which could partly transform to cubic $ZrWMoO_8$ after sintering at higher temperature (900 °C, Fig. 1c). The XRD pattern of powders synthesized at 1020 °C shown in Fig. 1d is identical to that of α-ZrW_2O_8, indicating that the room temperature structure of $ZrWMoO_8$ synthesized using in situ solid state method can be identified as a single phase having α-ZrW_2O_8 structure. This phenomenon is different with the literature [17, 18] which reports that the room temperature structure of $ZrWMoO_8$ is indexed as β-ZrW_2O_8 structure whose XRD pattern has no diffraction peaks (111), (221), (310), (410), and (331), and the different fabrication method utilized is speculated to be the reason. This study is the first paper reporting about $ZrWMoO_8$ with α-ZrW_2O_8 structure obtained at room temperature.

The other samples (G2, G3, G4, C1, C2, and C3) are calcined at 1020 °C, and the XRD patterns of the resulted products are shown in Fig. 2. The diffraction peaks of the composite sample fabricated using in situ solid state method could be indexed as either pure α-$ZrWMoO_8$ or ZrO_2's characteristic peaks, illustrating that the composition is

Table 2 The mass of raw materials applied in co-precipitation route

Sample	Composition	$N_5H_{37}W_6O_{24}\cdot H_2O$ (g)	$N_5H_{37}Mo_6O_{24}\cdot H_2O$ (g)	$ZrO(NO_3)_2\cdot 5H_2O$ (g)
C1	β-$ZrWMoO_8$	7.606	10.593	24.253
C2	β-$ZrWMoO_8$/50 wt% ZrO_2	3.803	2.648	19.957
C3	β-$ZrWMoO_8$/33 wt% ZrO_2	2.535	1.765	29.237

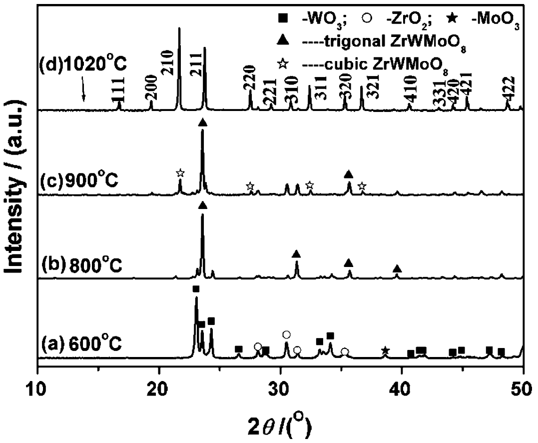

Fig. 1 XRD patterns of sample G1 calcined at different temperatures

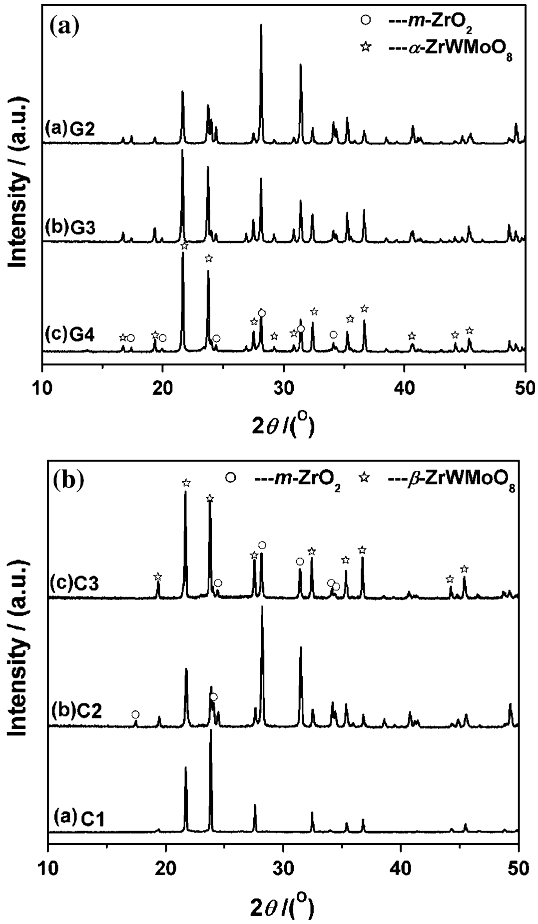

Fig. 2 XRD patterns of samples calcined at 1020 °C for 1.5 h using **a** in situ solid state reaction method and **b** co-precipitation route

α-$ZrWMoO_8$ and ZrO_2 without any impurities. Further observation can find that the peak intensities of α-$ZrWMoO_8$ and ZrO_2 are different from each other, which indicates different weight ratios of α-$ZrWMoO_8$ and ZrO_2 in the composites.

It is noteworthy that the XRD pattern of $ZrWMoO_8$ obtained by co-precipitation route is obviously different from that obtained by in situ solid state method. The disappearance of the diffraction peaks of (111), (221), (310), (410), and (331) shows that $ZrWMoO_8$ fabricated by co-precipitation route adopts the disordered β-ZrW_2O_8 structure. The composition of the composite samples fabricated using co-precipitation route can be characterized to be β-$ZrWMoO_8$ and ZrO_2. This result is in agreement with the previous study [16], where $ZrWMoO_8$ obtained using dehydration precursor method adopts β-ZrW_2O_8 structure at room temperature; therefore, the fabrication method was supposed to have a great influence on the structure of the resulted $ZrWMoO_8$. Solid materials were utilized as initial reaction material for solid state reaction method, while the other two methods (dehydration precursor method and the co-precipitation route) were both taken place in water solution which was testified to have an effect on the structure of $ZrWMoO_8$ [16]. It can be concluded that $ZrWMoO_8$ prepared without participating of water adopts α-ZrW_2O_8 structure at room temperature, otherwise, adopts β-ZrW_2O_8 structure. Based on these results, it can be inferred that the water must have an important effect in the reaction process and the structure of resulted products, and the detailed mechanism is still under researching and will be reported later.

The thermal expansion property of the composite was measured by TMA and presented in Fig. 3, and the specific values of the CTE were listed in Table 3. Compared with ZrO_2, all of the composites fabricated by the above two methods possess lower thermal expansion, suggesting that the addition of $ZrWMoO_8$ can decrease the thermal expansion effectively. Special attention should be paid to sample G2 and C3, both of them exhibit near zero thermal expansion property over the entire measurement temperature range. Figure 4 shows the SEM images of sample G2 and C3, it can be clearly seen that the composites prepared

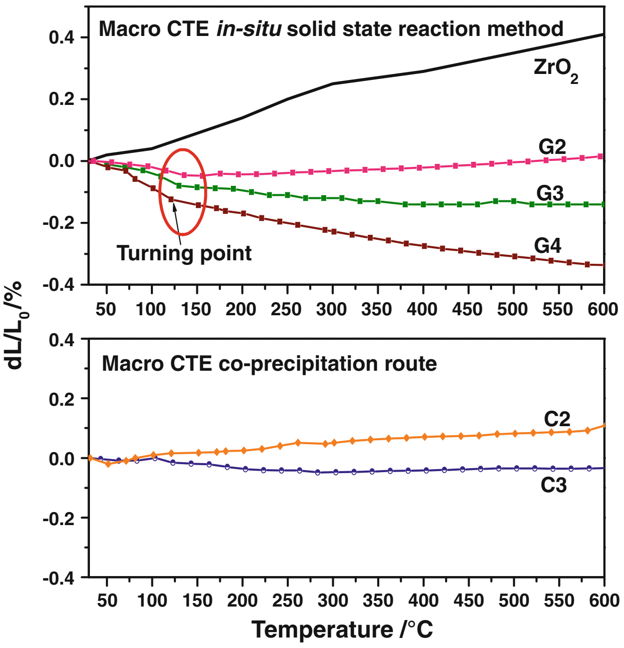

Fig. 3 Thermal expansion curves of composites

by in situ solid state method are micro-structurally different from the co-precipitation method. EDS results indicate that the larger one is $ZrWMoO_8$ and the smaller one is ZrO_2. Both of the samples are not dense due to the insufficient sintering of ZrO_2 which needed to be sintered at much higher temperatures (2100 °C) than $ZrWMoO_8$ (1020 °C).

What still deserves to be mentioned is an obvious difference among the thermal expansion curves of the composite samples prepared by different methods, a discontinuity around 150 °C exists in the curves of the composites prepared by in situ solid state method, while the others are linear. A similar discontinuity observed in the thermal expansion curves of ZrO_2/α-ZrW_2O_8 composites is confirmed to be caused by the α–β phase transition of α-ZrW_2O_8, so it is speculated that similar phase transition might occur in α-$ZrWMoO_8$ and lead to the variation of thermal expansion.

α-$ZrWMoO_8$ is tested by in situ XRD, and the results are shown in Fig. 5, it can be seen that (111), (221), (310), (410), and (331) peaks existing in the XRD pattern at room temperature are progressively decrease on warming and disappear at 150 °C. This behavior is same with that of the α–β phase transition of ZrW_2O_8, suggesting that α-$ZrWMoO_8$ transforms to β-phase at 150 °C. Besides that, the diffraction peaks slowly shrift to right during the temperature range from room temperature (r.t.) to 700 °C, which can be clearly seen in the partial enlarged drawing (Fig. 5b), this behavior confirms that α-$ZrWMoO_8$ contracts upon heating. Otherwise, the material is stable up to the temperatures lower than 700 °C, then it decomposes into triclinic WO_3, tetragonal MoO_3, and monoclinic ZrO_2 (Fig. 5c). The in situ XRD results [see Supporting Information, Figure S1 (a)] of β-$ZrWMoO_8$ (Sample C1) suggest that it retains disordered β structure throughout the temperature range from r.t. to 600 °C. Sample C1 is further calcined at 150 °C for 3 h and cooled in air, the resulted products [see Supporting Information, Figure S1 (b)] still adopt β-$ZrWMoO_8$ structure, these results mean that even

Table 3 Cell parameter and thermal expansion coefficient of sample G1 and C1

Sample	Cell parameter at r.t. (Å)	Micro CTE (× 10^{-6} °C^{-1})			Macro CTE (× 10^{-6} °C^{-1})		
		30–150 °C	150–600 °C	30–600 °C	30–150 °C	150–600 °C	30–600 °C
G1	9.152	−7.332	−4.156	−6.543	−8.143	−3.977	−5.944
C1	9.133	–	–	−4.672	–	–	−4.143

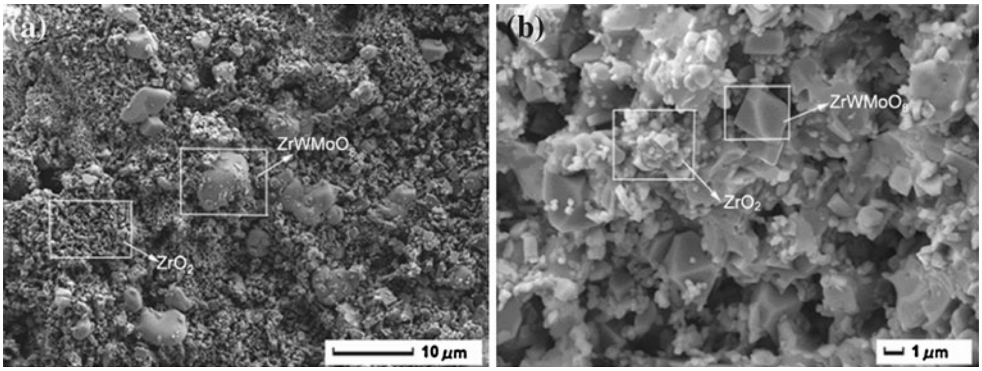

Fig. 4 SEM images of $ZrWMoO_8$ **a** G2 and **b** C3

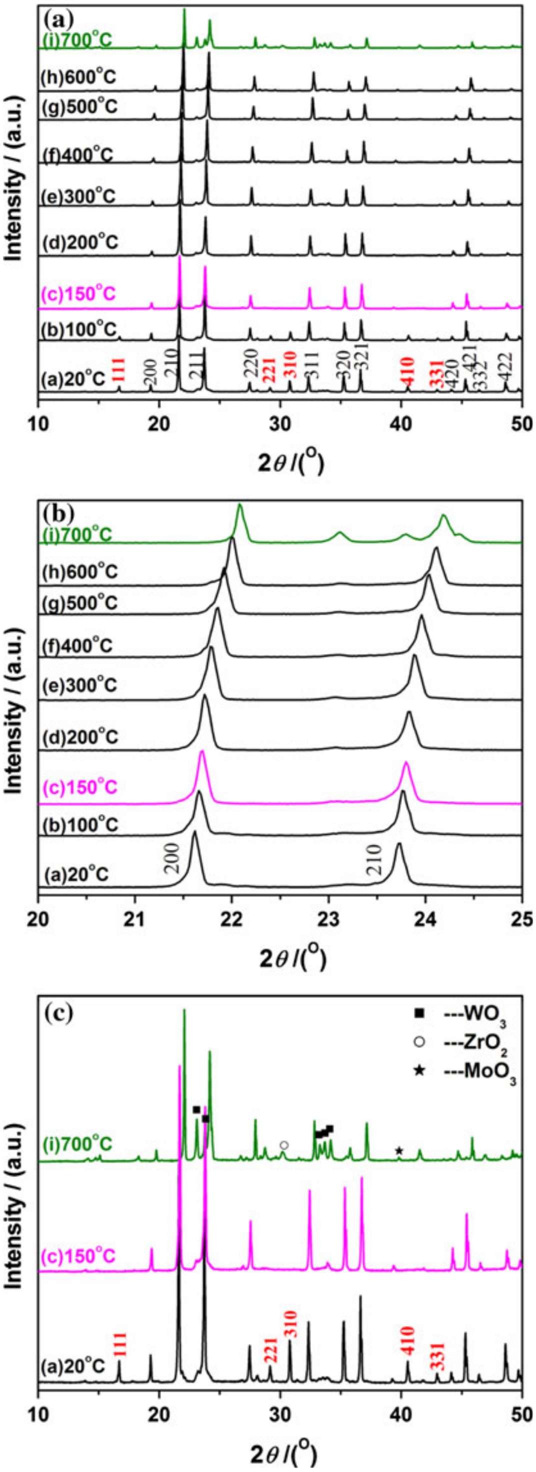

Fig. 5 XRD patterns of α-ZrWMoO$_8$ characterized at different temperatures

at 600 °C there is an unequivocal evidence of its stabilization.

Table 4 Thermal expansion coefficient of composites

Sample	Average thermal expansion coefficient (× 10^{-6} °C^{-1})		
	30–150 °C	150–600 °C	30–600 °C
G2	−3.302	1.312	0.472
G3	−4.356	−1.171	−2.017
G4	−4.654	−2.372	−3.437
C2	–	–	−0.61
C3	–	–	1.52

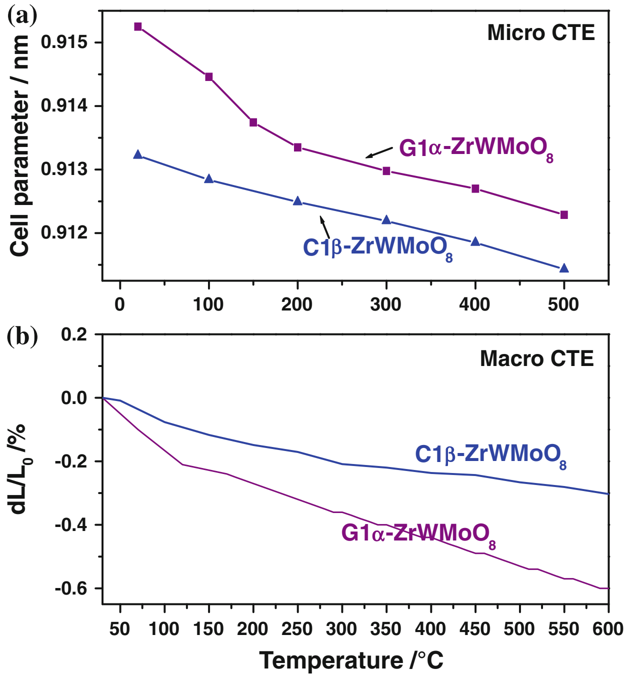

Fig. 6 **a** Micro and **b** macro thermal expansion curves of α-ZrWMoO$_8$ and β-ZrWMoO$_8$

Cell parameters of α and β-ZrWMoO$_8$ are calculated using the PowderX software, and the values at r.t. are given in Table 4. The cell parameter of β-ZrWMoO$_8$ correlated with the literature (9.147 Å) [18] is much smaller than that of α-ZrWMoO$_8$. The small differences between α and β phase can be explained by taking into account of the different directions of the W(Mo)O$_4$ tetrahedra lying along the threefold axis in the structure [19].

The micro CTE is calculated using the data of cell parameters of α and β-ZrWMoO$_8$ at different temperatures, the results are shown in Fig. 6 and listed in Table 4. On heating, a continuous contraction is observed for both of the samples. An apparent discontinuity existing in the thermal expansion curve for α-ZrWMoO$_8$ structure (around 150 °C) is due to the α–β phase transition, while the other is linear. The macro CTE curves exhibit the same behavior, and the slight difference of the data might be caused by the different testing methods. The results confirm that the existence of the α–β phase transition for α-ZrWMoO$_8$

causes the deviation of the thermal expansion curves of itself and its composites, which suggests that β-$ZrWMoO_8$ with linear CTE above room temperature may have greater practical importance as it can refraining from generating thermal mismatch stress caused by variation of CTE of the component material.

Conclusion

Preparation method has a great influence on the structure of the $ZrWMoO_8$, and the possible reason is that water may take part in the reaction process and thus influence the structure of resulted products. β-$ZrWMoO_8$ showing linear NTE property above room temperature only can be synthesized using co-precipitation route, it is an optimal addition to decrease the thermal expansion of ZrO_2 in practical application as it can avoid the thermal stress brought out by the α–β phase transition of α-$ZrWMoO_8$.

Acknowledgements The authors thank the National Natural Science Foundation of China (No. 50772044) and Doctoral Fund of Ministry of Education of China (No. 200802990001).

References

1. Ostertag W, Fischer GR, Williams JP (1968) J Am Ceram Soc 51:651
2. Schultz H (1974) J Am Ceram Soc 57:313
3. Buessem WR, Thielke NR, Sarakauskas RV (1952) Ceram Age 60:38
4. Mary TA, Evans JSO, Vogt T, Sleight AW (1996) Science 272:92
5. Pryde AKA, Hammonds KD, Dove MT, Heine V, Gale JD, Warren MC (1996) J Phys Condens Matter 8:10973
6. Sleight AW (1998) Inorg Chem 37:2854
7. Sun L, Sneller A, Kown P (2008) Compos Sci Technol 68:3425
8. Yang XB, Xu J, Li HJ, Li HJ, Cheng XN, Yan XH (2007) J Am Ceram Soc 90(6):1953
9. Evans JSO, Hu Z, Jorgensen JD, Argyriou DN, Short S, Sleight AW (1997) Science 275:61
10. Verdon C, Dunand DC (1997) Scr Mater 36(9):1075
11. Jakubinek MB, Whitman CA, White MA (2010) J Therm Anal Calorim 99(1):165
12. Evans JSO, Hanson PA, Ibberson RM, Duan N, Kameswari U, Sleight AW (2000) J Am Chem Soc 122:8694
13. Hampson MH, Allen S, King IJ, Crossland CJ, Hodgkinson P, Harris RK, Fayon F, Evans JSO (2005) Solid State Sci 7:819
14. Liu QQ, Yang J, Sun XJ, Cheng XN (2007) J Mater Sci 42(7):2528. doi:10.1007/s10853-007-1563-4
15. Closmann C, Sleight AW, Haygarth JC (1998) J Solid State Chem 139:424
16. Liu QQ, Yang J, Sun XJ, Cheng XN (2008) Phys status solidi b 245(11):2477
17. Mancheva M, Iordanova R, Dimitriev Y, Avdeev G (2009) J Non-Cryst Solids 355(37-42):1904
18. Kameswari U, Sleight AW, Evans JSO (2000) Int J Inorg Mater 2(4):333
19. Cao D, Bridges F, Kowach GR, Ramirez AP (2002) Phys Rev Lett 89(21):215902-1